Published in IET Microwaves, Antennas & Propagation
Received on 19th June 2012
Revised on 26th October 2012
Accepted on 4th December 2012
doi: 10.1049/iet-map.2012.0334

ISSN 1751-8725

# Improved reactance domain unitary propagator algorithms for electronically steerable parasitic array radiator antennas

*Salem Akkar, Ferid Harabi, Ali Gharsallah*

*Unit of Research in High Frequency Electronic Circuits and Systems, Faculty of Sciences of Tunis El Manar University, 2092, Tunisia*
*E-mail: salemakkar@yahoo.fr*

**Abstract:** In this study, the authors propose four algorithms for directions of arrival (DoAs) estimation of multiple incoming narrowband plane waves onto electronically steerable parasitic array radiator antennas. The constraints on the proposed algorithms are the same as those imposed onto the classic subspace methods allowing superior high-resolution and localisation capabilities even for correlated sources scenarios but with more reduced computations load and processing time than existing schemes. We also demonstrate that estimating the propagator operator through both introduced real-valued orthogonal decompositions techniques not only yields to a faster DoAs estimation with a reduced computational complexity, but also it improves the robustness of the developed algorithms to noise as compared with the classic propagator algorithm. The Cramér–Rao bound on the variance of the estimated DoAs by the proposed algorithms is analysed. The achieved performance by the developed methods is studied and compared with conventional antenna arrays. The simulation results confirm that high-resolution DoAs estimation can be achieved with the developed algorithms and prove the validity of the proposed approach.

## 1 Introduction

Reducing both energetic consumption and calculation complexity is a challenging topic that has attracted considerable attentions in wireless communication systems. Recently, researchers have developed various high-resolution directions of arrival (DoAs) estimators based on the eigendecomposition of the array covariance matrix (CM) such as multiple signal classification (MUSIC), estimation of signal parameters via rotational invariance techniques (ESPRIT) and propagator [1–4]. Particularly, based on the reactance domain (RD) technique, a great deal of efforts and literatures [5–8] has been focused on taking advantages from electronically steerable parasitic antennas radiator (ESPAR) to improve performances of localisation systems via high-resolution methods such as unitary RD-MUSIC [5], RD-MUSIC [6] and RD-ESPRIT [7]. This kind of antennas arrays is composed of one active (fed) element surrounded by some parasitic elements. Fundamentally based on the mutual coupling, ESPAR antenna arrays are free from the negative influences of this phenomenon, which allows us to have smaller array-size. In addition, other advantages over conventional arrays include the low-power consumption (only the active element is fed), a low cost (only one receiver chain placed in the output of the active element) and an easy fabrication. All these advantages make the ESPAR antennas very suitable for wireless applications such as mobile user terminals in *ad-hoc* networks because of the reduced energy consumption usually demanded in such applications. In order to ensure high DoAs estimation accuracy with a low computational complexity, this paper proposes four algorithms that were not applied to an ESPAR antenna before. The first algorithm, namely the Reactance Domain propagator algorithm (RD-PM), is a direct formulation of the standard propagator method (PM) to the ESPAR antennas systems and has the advantage of requiring only linear operations to perform an accurate DoAs estimation. However, the second algorithm, namely the unitary RD PM (Unit-RD-PM), is a real-valued formulation of the RD-PM algorithm by means of unitary transformation of the estimated RD-CM. Therefore the computational efforts are saved because all tasks can be accomplished by real computations and both calculation cost and complexity are reduced by at least a factor of four since the cost of real multiplication is four times lesser than complex multiplication. Moreover, since the unitary transformation of the RD-CM incorporates forward–backward averaging, that effectively doubles the number of snapshots (samples), the resolution capability of the DoAs estimator is further improved. To further reduce the calculation cost and complexity without sacrificing DoAs estimation accuracy, we also propose two other algorithms, in this paper, namely the unitary LU-RD-propagator algorithm and the unitary QR-RD-propagator algorithm. These two algorithms are based on two real-valued orthogonal decompositions

(RVOD) techniques to estimate the real-valued propagator operator and both are very efficient in noisy situations. The key idea is to apply one of the RVOD techniques, such as the ***QR*** decomposition or the ***LU*** decomposition, to estimate the real-valued propagator operator from the estimated real-valued sample covariance matrices. These orthogonal decomposition techniques [9–11] are useful tools commonly used in linear algebra to find solutions for linear equations. On the other hand, because both algorithms also use real-valued covariance matrices, the necessary information about the propagator operator is obtained through real-valued ***QR*** orthogonal decomposition or real-valued ***L***ower triangular matrix and ***U***pper triangular matrix (***LU***) orthogonal decomposition without loss of the unit-RD-PM algorithm advantages aforementioned.

The paper outline is as follows. In Section 2, we describe the ESPAR antennas signal model. Section 3 presents the development of the proposed algorithms. In Section 4, the performances of the proposed methods are analysed and discussed via computer simulations. In Section 5, we draw our conclusions.

The superscripts $(.)^{\mathrm{T}}$, $(.)^{*}(.)^{\mathrm{H}}$, $(.)^{-1}$ and $(.)^{\dagger}$ are the matrix transpose, conjugate, Hermitian, inverse and the Moore–Penrose pseudo-inverse operators, respectively. However, $\Re(\cdot)$ is the real-part extraction operators and $\boldsymbol{I}_M$ is the $M$-order identity matrix.

## 2 Problem formulation

The ESPAR antennas configuration is composed of one fed active element (#0) surrounded by $M=6$ parasitic radiating elements (#1–#6) of length $l=\lambda/4$ placed in the near-field of the active radiator as illustrated in Fig. 1. The six parasitic elements are connected to the ground plane via some variable reactances $\{x_m\}_{m=1}^{M}$ used to modify the radiation patterns of the ESPAR antennas by adjusting their values. We take the active element as the reference and we denote by $r=\lambda/4$ its radius, where the sources wavelength is denoted by $\lambda$. In the presence of $K$ narrowband uncorrelated signals (i.e. $\forall i \neq j$, $E[s_i s_j^*]=0$) from $K$ distinct DoAs ($\theta_1, \theta_2, \ldots, \theta_K$) the steering matrix is given as

$$\boldsymbol{A}=[\boldsymbol{a}(\theta_1), \boldsymbol{a}(\theta_2), \ldots, \boldsymbol{a}(\theta_K)] \tag{1}$$

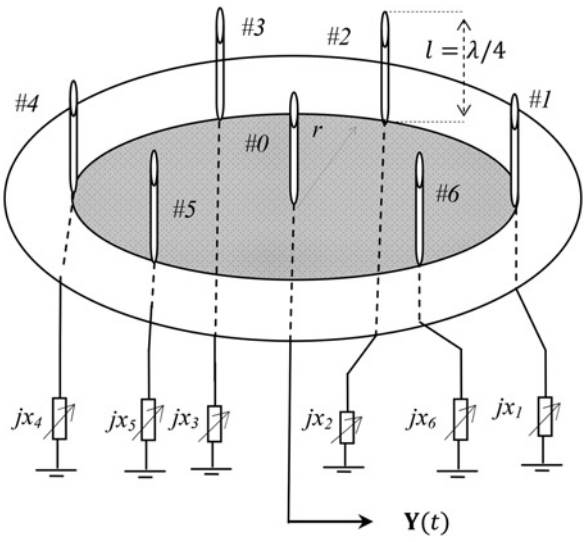


**Fig. 1** *Seven-element ESPAR antennas*

where $\boldsymbol{a}(\theta_k)=[1, e^{j\frac{\pi}{2}\cos(\theta_k-\varphi_1)}, \ldots, e^{j\frac{\pi}{2}\cos(\theta_k-\varphi_M)}]^{\mathrm{T}}$ and $\psi_m=2\pi/M(m-1)$, for $m=1$ to $M$.

Since the data are available only in the output of the active element, an additional assumption about sources is required to estimate the RD-CM. Indeed, the $K$ incident sources are assumed to be sent periodically from the far-field. Therefore the spatial diversity of conventional arrays is recreated by periodically changing the reactance value and, thus, the radiation patterns of the ESPAR antennas. While the signals are periodically sent, as many times as the used directional radiation patterns (e.g. $M+1$ times), the received signals from the output of the active element $y(t_m)$ is saved into a vector $\boldsymbol{Y}$. The assumption of periodic signals allows us to write

$$S_k(t_1)=S_k(t_2)=\cdots=S_k(t_{M+1}) \tag{2}$$

where $S_k(t_m)$ is the complex magnitude of the $k$th incoming periodic signal at instant time $t_m$.

By changing the reactances value of parasitic elements under $M+1$ periods (accordingly we change the radiation patterns of the ESPAR antennas $M+1$ times), we can get our data vector $\boldsymbol{Y}(t)\in\mathbb{C}^{(M+1)\times(1)}$. Thus, we can have several observations of the same radiated field but with different ESPAR antennas radiation patterns. This technique is known in signal processing as the RD technique [6].

The received signal vector $\boldsymbol{Y}(t)$ from the ESPAR antennas can be written as

$$\boldsymbol{Y}(t)=[y(t_1), y(t_2), \ldots, y(t_{M+1})]^{\mathrm{T}} \tag{3}$$

where $y(t_m)=\sum_{k=1}^{K}\boldsymbol{w}_m^{\mathrm{T}}\boldsymbol{a}(\theta_k)S_k(t_m)+n(t_m)$.

The frequency-weighted matrix $\boldsymbol{W}$ is given as

$$\boldsymbol{W}=[\boldsymbol{w}_1^{\mathrm{T}}, \boldsymbol{w}_2^{\mathrm{T}}, \ldots, \boldsymbol{w}_{M+1}^{\mathrm{T}}]^{\mathrm{T}} \tag{4}$$

Each component of $\boldsymbol{W}$ is computed as

$$\boldsymbol{w}_m=2Z_s(\boldsymbol{Z}+\boldsymbol{X}^{(m)})^{(-1)}\boldsymbol{u} \tag{5}$$

with $Z_s$ is the receiver's input impedance, $\boldsymbol{u}=[1, 0, 0, \ldots, 0]^{\mathrm{T}}$, $\boldsymbol{Z}\in\mathbb{C}^{(M+1)\times(M+1)}$ is the mutual impedances matrix and $\boldsymbol{X}^{(m)}$ is a diagonal matrix containing the $m$th set of reactance ($m=1$ to $M+1$) given as

$$\boldsymbol{X}^{(m)}=\mathrm{diag}\{Z_s, jx_1^{(m)}, jx_2^{(m)}, \cdots, jx_M^{(m)}\} \tag{6}$$

As in conventional arrays, the received data vector in matrix notation is written as

$$\boldsymbol{Y}(t)=\boldsymbol{W}^{\mathrm{T}}\boldsymbol{A}\boldsymbol{S}(t)+\boldsymbol{N}(t) \tag{7}$$

However, the CM is given as

$$\boldsymbol{R}_{yy}=E[\boldsymbol{Y}\boldsymbol{Y}^{\mathrm{H}}]=\boldsymbol{W}^{\mathrm{T}}\boldsymbol{A}\boldsymbol{R}_s\boldsymbol{A}^{\mathrm{H}}\boldsymbol{W}^{*}+\boldsymbol{R}_n \tag{8}$$

where $\boldsymbol{R}_s=E[\boldsymbol{S}\boldsymbol{S}^{\mathrm{H}}]$ denotes the signals CM, $\boldsymbol{N}(t)=[n(t_1), n(t_2), \ldots, n(t_{M+1})]^{\mathrm{T}}$ refers to an additive Gaussian noise assumed to be spatially white, uncorrelated and zero mean, $E[\boldsymbol{N}\boldsymbol{N}^{H}]=\boldsymbol{R}_n=\sigma^2 I$ is the noise CM and $\sigma^2$ is the noise power. We also assume that the noise and




doi: 10.1049/iet-map.2012.0334

the signals are uncorrelated with each other (e.g. $\forall i, j$; $E[s_i n_j^*] = 0$). In practice case, only an estimate of the RD-CM is available, which can be obtained through $N_s$ snapshots as

$$\widehat{\boldsymbol{R}}_{yy} = \frac{1}{N_s}\sum_{i=1}^{N_s} \boldsymbol{Y}\boldsymbol{Y}^{\mathrm{H}} \tag{9}$$

## 3 Development of the proposed methods

Based on the standard propagator methods [3], we present in this section four non-eigenvector algorithms for DoAs estimation with ESPAR antennas. Hereinafter, the frequency-weighted matrix $\boldsymbol{W}$ is assumed full rank for the chosen reactance sets and perfectly known or obtained through experimental measurement or calculated using (5) jointly with a mutual impedance extraction technique [8]. The sources number $K$ is assumed to be known or has been perfectly estimated by the AIC or MDL criteria addressed in [12].

### 3.1 RD-propagator algorithm

The propagator method is based on the partition of the steering matrix $\boldsymbol{A}$. As in common subspace methods, we assume that the RD-steering matrix $\boldsymbol{A}_{\mathrm{RD}} = \boldsymbol{W}^{\mathrm{T}}\boldsymbol{A}$ is full rank (i.e. $\mathrm{rank}(\boldsymbol{A}_{\mathrm{RD}}) = K$) for the chosen reactances sets and that its first rows are linearly independent. In this case, there exists an $(M+1-K)\times K$ matrix $\boldsymbol{P}$ called the propagator operator [3] such that

$$\bar{\boldsymbol{A}}_2 = \boldsymbol{P}\bar{\boldsymbol{A}}_1 \tag{10}$$

where $\bar{\boldsymbol{A}}_1$ and $\bar{\boldsymbol{A}}_2$ are the $(K\times K)$ and the $(M+1-K)\times K$ sized block matrices, respectively, obtained by partitioning the RD steering matrix as $\boldsymbol{A}_{\mathrm{RD}} = [\bar{\boldsymbol{A}}_1^{\mathrm{T}}\ \bar{\boldsymbol{A}}_2^{\mathrm{T}}]^{\mathrm{T}}$.

If we define the $(M+1)\times K$ matrix $\boldsymbol{E}_p$ as $\boldsymbol{E}_p = [\boldsymbol{P}^{\mathrm{T}}\ -\boldsymbol{I}_{M+1-K}]^{\mathrm{T}}$, we have $\boldsymbol{E}_p^{\mathrm{H}}\boldsymbol{A}_{\mathrm{RD}} = \boldsymbol{P}\bar{\boldsymbol{A}}_1 - \bar{\boldsymbol{A}}_2 = \boldsymbol{0}$. In other words, the $(M+1)\times K$ columns of matrix $\boldsymbol{E}_p$ are orthogonal to the columns of steering matrix $\boldsymbol{A}_{\mathrm{RD}}$. This means that the subspace spanned by the columns of the matrix $\boldsymbol{E}_p$ is the same as the subspace spanned by the noise subspace obtained through an eigendecomposition of the data CM $\widehat{\boldsymbol{R}}_{yy}$. It follows that the DoAs can be taken as the directions that minimise the so-called spatial spectrum function given as

$$\hat{\theta}_k = \min_{\theta}\|\hat{\boldsymbol{E}}_p\boldsymbol{W}^{\mathrm{T}}\boldsymbol{a}(\theta)\|^2 \tag{11}$$

Note that the introduced RD-PM is based on the noise subspace spanned by the columns of matrix $\hat{\boldsymbol{E}}_p$, where its computation requires a-prior knowledge of matrix $\boldsymbol{A}_{\mathrm{RD}}$ that is usually unknown. However, matrix $\hat{\boldsymbol{E}}_p$ can be estimated only from the received data using the least-square solution as will be more explained in Section 3.3.

### 3.2 Real-valued RD-CM

To take more advantages from the Centro-symmetric geometry of the ESPAR antennas and enhance DoAs estimation capabilities, we transform the estimated RD-CM (9) to a real-valued representation that virtually doubles the snapshots number and decorrelates possible correlated sources. To achieve this goal, the Centro-Hermitian property of the resulting RD-CM (9) is forced by means of the so-called forward–backward averaging (FBA) technique [13]. However, because of the specific geometry of our ESPAR antennas, components of $\widehat{\boldsymbol{R}}_{yy}$ must first be arranged to have Centro-Hermitian form (linear order) as follows

$$\widehat{\boldsymbol{R}}_a = \boldsymbol{T}\widehat{\boldsymbol{R}}_{yy}\boldsymbol{T}^{\mathrm{T}} \in \mathbb{C}^{(M+1)\times(M+1)} \tag{12}$$

with $\boldsymbol{T}$ is an $(M+1)$-order square transform matrix composed of zeros and ones satisfying $\boldsymbol{T}^{\mathrm{T}}\boldsymbol{T} = \boldsymbol{I}$ and given as

$$\boldsymbol{T} = \begin{bmatrix} 0 & 1 & 0 & 0 & 0 & 0 & 0 \\ 0 & 0 & 1 & 0 & 0 & 0 & 0 \\ 0 & 0 & 0 & 0 & 0 & 0 & 1 \\ 1 & 0 & 0 & 0 & 0 & 0 & 0 \\ 0 & 0 & 0 & 1 & 0 & 0 & 0 \\ 0 & 0 & 0 & 0 & 0 & 1 & 0 \\ 0 & 0 & 0 & 0 & 1 & 0 & 0 \end{bmatrix} \tag{13}$$

Then, instead of the conventional (forward-only) RD-CM, the FBA-RD-CM can be obtained as

$$\widehat{\boldsymbol{R}}^{\mathrm{FBA}} = \frac{1}{2}(\widehat{\boldsymbol{R}}_a + \boldsymbol{J}\widehat{\boldsymbol{R}}_a^*\boldsymbol{J}) \in \mathbb{C}^{\times(M+1)} \tag{14}$$

where $\boldsymbol{J}$ is the exchange matrix with zeros components except in its anti-diagonal.

On the other hand, since the inner product between any two conjugate Centro-symmetric vectors is real-valued, any matrix of which each row is conjugate Centro-symmetric may be employed to transform the complex-valued element into a real-valued one. However, as mentioned by numerous authors [14, 15], the simplest matrices for accomplishing that are $\boldsymbol{Q}_n$ and $\boldsymbol{Q}_{2n+1}$ defined as follows

$$\boldsymbol{Q}_M = \begin{cases} \dfrac{1}{\sqrt{2}}\begin{bmatrix} \boldsymbol{I}_{(M-1/2)} & \boldsymbol{0}_{(M-1/2)} & j\boldsymbol{I}_{(M-1/2)} \\ \boldsymbol{0}_{(M-1/2)}^{\mathrm{T}} & \sqrt{2} & \boldsymbol{0}_{(M-1/2)}^{\mathrm{T}} \\ \boldsymbol{J}_{(M-1/2)} & \boldsymbol{0}_{(M-1/2)} & -j\boldsymbol{J}_{(M-1/2)} \end{bmatrix} & \text{for odd } M \\ \dfrac{1}{\sqrt{2}}\begin{bmatrix} \boldsymbol{I}_{(M/2)} & j\boldsymbol{I}_{(M/2)} \\ \boldsymbol{J}_{(M/2)} & -j\boldsymbol{J}_{(M/2)} \end{bmatrix} & \text{for even } M \end{cases} \tag{15}$$

where $\boldsymbol{I}_M$ denotes the $\boldsymbol{M}$-order identity matrix and $\boldsymbol{0}_M$ is the $\boldsymbol{M}$-order zero vector.

We introduce the real-valued RD-CM defined [16] as

$$\boldsymbol{R}_u = \boldsymbol{Q}_{M+1}^{\mathrm{H}}\boldsymbol{R}^{\mathrm{FBA}}\boldsymbol{Q}_{M+1} \tag{16}$$

However, the estimated one can be given as

$$\widehat{\boldsymbol{R}}_u = \frac{1}{2}(\boldsymbol{Q}_{M+1}^{\mathrm{H}}\widehat{\boldsymbol{R}}_a\boldsymbol{Q}_{M+1} + \boldsymbol{Q}_{M+1}^{\mathrm{H}}\boldsymbol{J}\widehat{\boldsymbol{R}}_a^*\boldsymbol{J}\boldsymbol{Q}_{M+1}) \tag{17}$$

Using the fact that $\boldsymbol{J}\boldsymbol{Q}_{M+1}^* = \boldsymbol{Q}_{M+1}$ and $\boldsymbol{J}^{\mathrm{H}} = \boldsymbol{J}$, (17) becomes

$$\widehat{\boldsymbol{R}}_u = \frac{1}{2}(\boldsymbol{Q}_{M+1}^{\mathrm{H}}\widehat{\boldsymbol{R}}_a\boldsymbol{Q}_{M+1} + (\boldsymbol{Q}_{M+1}^{\mathrm{H*}})^{\mathrm{H}}\widehat{\boldsymbol{R}}_a^*\boldsymbol{Q}_{M+1}) \tag{18}$$

From (18), we show that matrix $\widehat{\boldsymbol{R}}_u$ can be directly estimated from the arranged forward-only RD-CM (12) as

$$\widehat{\boldsymbol{R}}_u = \Re\{\boldsymbol{Q}_{M+1}^{\mathrm{H}} \widehat{\boldsymbol{R}}_a \boldsymbol{Q}_{M+1}\} \in \mathbb{R}^{(M+1)\times(M+1)} \tag{19}$$

From (19), we show that all computations can now be done with real-valued matrices, which form the basis of our proposed unit-RD-PM algorithm. Based on (18) and (19), it can be readily shown that the FBA is achieved by transforming the complex components data CM $\widehat{\boldsymbol{R}}_{yy}$ into a real-valued matrix $\widehat{\boldsymbol{R}}_u$ after arrangement of their components into linear form according to (12). Moreover, since (19) proves that the real-valued RD-CM estimated from the forward-only RD-CM is equivalent to those estimated from the FBA-RD-CM (14), our proposed algorithms can be applied to coherent sources scenarios. In addition, estimating the real-valued RD-CM through the forward-only RD-CM not only yields to a very low computational cost methodology with a reduced data storage requirements, but also, it avoids certain degradations of asymptotic performances caused by the FBA technique [16].

### 3.3 Unit-RD-propagator algorithm

Our development starts with the definition of a new real-valued RD-steering matrix as

$$\boldsymbol{A}_e = \boldsymbol{Q}_{M+1}^{\mathrm{H}} \boldsymbol{T}\boldsymbol{W}^{\mathrm{T}} \boldsymbol{A} = \begin{bmatrix} \boldsymbol{A}_1 \\ \cdots \\ \boldsymbol{A}_2 \end{bmatrix} \begin{matrix} \}_K \\ \\ \}_{M+1-K} \end{matrix} \tag{20}$$

As in common subspace methods, we assume that this new steering matrix $\boldsymbol{A}_e$ has full rank (i.e. $\mathrm{rank}(\boldsymbol{A}_e) = K$), which means that it has $K$-independent rows. Let $\boldsymbol{A}_1$ be a square submatrix containing these $K$-independent rows. The real-valued propagator operator $\boldsymbol{P}_u \in \mathbb{R}^{K\times M+1-K}$ is defined as the unique real-valued linear operator [3] satisfying

$$\boldsymbol{P}_u^{\mathrm{H}} \boldsymbol{A}_1 = \boldsymbol{A}_2 \tag{21}$$

However, since our data model include noisy situations, we first partition the real-valued RD-CM (19) as

$$\widehat{\boldsymbol{R}}_u = \begin{bmatrix} \widehat{\boldsymbol{G}}_1 & \widehat{\boldsymbol{H}}_1 \\ \widehat{\boldsymbol{G}}_2 & \widehat{\boldsymbol{H}}_2 \end{bmatrix} \tag{22}$$

where

$$\begin{cases} \widehat{\boldsymbol{G}}_1 = \boldsymbol{A}_1 \boldsymbol{R}_s \boldsymbol{A}_1^{\mathrm{H}} + \hat{\sigma}^2 \boldsymbol{I}_K; & \in \mathbb{R}^{K\times K} \\ \widehat{\boldsymbol{H}}_2 = \boldsymbol{A}_2 \boldsymbol{R}_s \boldsymbol{A}_2^{\mathrm{H}} + \hat{\sigma}^2 \boldsymbol{I}_{M+1-K}; & \in \mathbb{R}^{M+1-K\times M+1-K} \\ \widehat{\boldsymbol{G}}_2 = \boldsymbol{A}_2 \boldsymbol{R}_s \boldsymbol{A}_1^{\mathrm{H}}; & \in \mathbb{R}^{M+1-K\times K} \\ \widehat{\boldsymbol{H}}_1 = \boldsymbol{A}_1 \boldsymbol{R}_s \boldsymbol{A}_2^{\mathrm{H}}; & \in \mathbb{R}^{K\times M+1-K} \end{cases} \tag{23}$$

After that, an estimation of the noise power can be made as

$$\hat{\sigma}^2 = \Re\left(\frac{\mathrm{tr}(\hat{\boldsymbol{\Pi}}_2 \hat{\boldsymbol{\Pi}})}{\mathrm{tr}(\hat{\boldsymbol{\Pi}})}\right) \tag{24}$$

where $\hat{\boldsymbol{\Pi}} = \boldsymbol{I}_{M+1-K} - \hat{\boldsymbol{G}}_2 \hat{\boldsymbol{G}}_2^{\dagger}$ and $\mathrm{tr}\{.\}$ denotes the trace operator.

Once the noise power $\hat{\sigma}^2$ is estimated, the noise CM $\widehat{\boldsymbol{R}}_n = \hat{\sigma}^2 \boldsymbol{I}$ can be retrenched from the estimated real-valued RD-CM, which allows us also to eliminate the mutual coupling effects as

$$\widehat{\boldsymbol{R}}_e = (\boldsymbol{Q}_{M+1}^{\mathrm{H}} \boldsymbol{T}\boldsymbol{W}^{\mathrm{T}})^{-1} (\widehat{\boldsymbol{R}}_u - \widehat{\boldsymbol{R}}_n)(\boldsymbol{Q}_{M+1}^{\mathrm{H}} \boldsymbol{T}\boldsymbol{W}^{\mathrm{T}})^{\mathrm{H}-1} \tag{25}$$

From (25), it is clear that the resulting data CM $\widehat{\boldsymbol{R}}_e$ resembles the data CM obtained in the noise-free case without mutual coupling. Thus, as in conventional antennas arrays, we can apply the formula of the partitioned inverse [16].

$$\widehat{\boldsymbol{R}}_e = [\widehat{\boldsymbol{G}} \quad : \quad \widehat{\boldsymbol{H}}] \tag{26}$$

According to the propagator definition, given in (21), we can write

$$\widehat{\boldsymbol{H}} = \widehat{\boldsymbol{G}} \widehat{\boldsymbol{P}}_u \tag{27}$$

However, relation (27) may not be satisfied in practice case since the actual RD-CM is estimated from a finite number of snapshots according to (9). Nevertheless, a least-square solution can be used to estimate $\widehat{\boldsymbol{P}}_u$ by minimisation of the following cost function

$$J(\widehat{\boldsymbol{P}}) = \|\widehat{\boldsymbol{H}} - \widehat{\boldsymbol{G}} \widehat{\boldsymbol{P}}_u\|_{\mathrm{F}}^2 \tag{28}$$

where $\|.\|_{\mathrm{F}}$ denotes the Frobenius norm.

The cost function $J(\widehat{\boldsymbol{P}}_u)$ given in (28) seems to be quadratic function of $\widehat{\boldsymbol{P}}_u$ and may be minimised to give the unique least-square solution for $\widehat{\boldsymbol{P}}_u$ as

$$\widehat{\boldsymbol{P}}_u = \widehat{\boldsymbol{G}}^{\dagger} \widehat{\boldsymbol{H}} \tag{29}$$

Based on (29), we define the matrix $\widehat{\boldsymbol{E}}$ as

$$\widehat{\boldsymbol{E}} \triangleq [\widehat{\boldsymbol{P}}_u, \ -\boldsymbol{I}_{M+1-K}]^{\mathrm{T}} \tag{30}$$

According to Marcos *et al.* [3], the subspace spanned by the columns of matrix $\widehat{\boldsymbol{E}}$ is orthogonal to those of the RD-steering matrix $\boldsymbol{A}_e$ which allow us to write

$$\boldsymbol{A}_e^{\mathrm{H}} \widehat{\boldsymbol{E}} = 0 \tag{31}$$

To ensure more DoAs estimation accuracy and enhance resolution capabilities of the proposed unit-RD-PM, $\widehat{\boldsymbol{E}}$ matrix components must be orthonormalised as

$$\widehat{\boldsymbol{E}}_n = \widehat{\boldsymbol{E}} (\widehat{\boldsymbol{E}}^{\mathrm{H}} \widehat{\boldsymbol{E}})^{-1/2} \tag{32}$$

Finally, the estimated DoAs are taken as the directions that minimise the following cost function




doi: 10.1049/iet-map.2012.0334

$$\hat{\theta}_k = \min_\theta \|\widehat{\boldsymbol{E}}_n \boldsymbol{Q}_{M+1}^{\mathrm{H}} \boldsymbol{T}\boldsymbol{a}(\theta)\|^2 \tag{33}$$

We report here that since the unit-RD-PM algorithm search function operates with real-valued data, the calculation complexity and the processing time are four times lower than the RD-MUSIC [6]. Moreover, the particularity of using only linear operations on the estimated RD-CM (instead of an eigendecomposition), as well as the possibility of adaptive implementation give our unit-RD-PM a potential interest for real-time implementations.

### 3.4 Improved unitary-RD propagator algorithms

In practice case, the signal-to-noise-ratio (SNR) value is not always high which involves that the performance of the propagator method will strongly depend on the signal information contained in the block matrix $\widehat{\boldsymbol{G}}_1$ with respect to the noise and its linear dependency with the block $\widehat{\boldsymbol{H}}_1$. To improve its robustness to noise, we propose to insert an orthogonal decomposition step within the unitary RD-PM algorithm described above. The key idea is to use the $\boldsymbol{LU}$ or the $\boldsymbol{QR}$ orthogonal decomposition as well as the properties of the upper triangular matrix to estimate the real-valued propagator operator. According to the $\boldsymbol{QR}$ decomposition theorem, the real-valued RD-CM (19) can be expressed as

$$\begin{aligned} \boldsymbol{R}_u = \boldsymbol{q}\boldsymbol{r} &= \begin{bmatrix} \boldsymbol{q}_{11} & \boldsymbol{0} \\ \boldsymbol{q}_{21} & \boldsymbol{I}_{M+1-K} \end{bmatrix} \begin{bmatrix} \boldsymbol{r}_{11} & \boldsymbol{r}_{12} \\ \boldsymbol{0} & \boldsymbol{r}_{22} \end{bmatrix} \\ &= \begin{bmatrix} \boldsymbol{q}_{11}\boldsymbol{r}_{11} & \boldsymbol{q}_{11}\boldsymbol{r}_{12} \\ \boldsymbol{q}_{21}\boldsymbol{r}_{11} & \boldsymbol{q}_{21}\boldsymbol{r}_{12} + \boldsymbol{r}_{22} \end{bmatrix} \end{aligned} \tag{34}$$

where $\boldsymbol{r}_{11} \in \mathbb{R}^{K\times K}$, $\boldsymbol{r}_{22} \in \mathbb{R}^{(M-K+1)\times(M-K+1)}$ are both real-valued upper triangular matrices and $\boldsymbol{r}_{12} \in \mathbb{R}^{(K)\times(M-K+1)}$ is a real-valued matrix.

From (21)–(23) and (34), we can write

$$\begin{cases} \boldsymbol{q}_{11}\boldsymbol{r}_{11} = \boldsymbol{A}_1 \boldsymbol{r}_s \boldsymbol{A}_1^{\mathrm{H}} + \sigma^2 \boldsymbol{I}_K; & \in \mathbb{R}^{K\times K} \\ \boldsymbol{q}_{21}\boldsymbol{r}_{12} + \boldsymbol{r}_{22} = \boldsymbol{A}_2 \boldsymbol{r}_s \boldsymbol{A}_2^{\mathrm{H}} + \sigma^2 \boldsymbol{I}_{M+1-K}; & \in \mathbb{R}^{M+1-K\times M+1-K} \\ \boldsymbol{q}_{21}\boldsymbol{r}_{11} = \boldsymbol{A}_2 \boldsymbol{r}_s \boldsymbol{A}_1^{\mathrm{H}}; & \in \mathbb{R}^{M+1-K\times K} \\ \boldsymbol{q}_{11}\boldsymbol{r}_{12} = \boldsymbol{A}_1 \boldsymbol{r}_s \boldsymbol{A}_2^{\mathrm{H}}; & \in \mathbb{R}^{K\times M+1-K} \end{cases} \tag{35}$$

Substituting (21) into (35) yields to

$$\boldsymbol{q}_{11}\boldsymbol{r}_{11} = \boldsymbol{q}_{11}\boldsymbol{r}_{12}\boldsymbol{P}_{QR} \tag{36}$$

According to (36), the novel estimate of the propagator operator using the $\boldsymbol{QR}$ decomposition is given as

$$\boldsymbol{P}_{QR} = \boldsymbol{r}_{11}^{-1}\boldsymbol{r}_{12} \tag{37}$$

From (37) we show that the useful signal components are concentrated in matrices $\boldsymbol{r}_{11}$ and $\boldsymbol{r}_{12}$. In other words, it concentrates the signal information, which is scattered in all the RD-CM elements. This concentration improves the robustness to noise of both proposed unitary RVOD-based propagator algorithms compared with the case where the classic propagator method is applied.

Following the similar formulation, using the $\boldsymbol{LU}$ decomposition, with the same partitioning in matrices $\boldsymbol{L}$ and $\boldsymbol{U}$, instead of matrices $\boldsymbol{q}$ and $\boldsymbol{r}$, we obtain the estimate propagator operator using the $\boldsymbol{LU}$ decomposition as

$$\boldsymbol{P}_{\mathrm{LU}} = \boldsymbol{U}_{11}^{-1}\boldsymbol{U}_{12} \tag{38}$$

Let $\boldsymbol{E}_{\mathrm{LU}} = [\boldsymbol{P}_{\mathrm{LU}}, -\boldsymbol{I}_{M+1-K}]^{\mathrm{T}}$ and $\boldsymbol{E}_{QR} = [\boldsymbol{P}_{QR}, -\boldsymbol{I}_{M+1-K}]^{\mathrm{T}}$ be the estimated noise subspace matrices obtained through the $\boldsymbol{LU}$ decomposition and the $\boldsymbol{QR}$ decomposition respectively. It follows that the estimated DoAs are given as the directions of arrival that minimise the following spectrum functions

$$\theta_k = \min_\theta \|\widehat{\boldsymbol{E}}_{QR} \boldsymbol{Q}_{M+1}^{\mathrm{H}} \boldsymbol{T}\boldsymbol{a}(\theta)\|^2 \tag{39}$$

$$\theta_k = \min_\theta \|\widehat{\boldsymbol{E}}_{LU} \boldsymbol{Q}_{M+1}^{\mathrm{H}} \boldsymbol{T}\boldsymbol{a}(\theta)\|^2 \tag{40}$$

Both proposed unit-RVOD-RD-Propagator algorithms are based on the $\boldsymbol{LU}$ or $\boldsymbol{QR}$ decomposition which requires considerably less computations than the standard eigendecomposition. Moreover, the useful signal components are concentrated in both upper triangular submatrices which yields to a better robustness to noise compared with the classical propagator method. Moreover, the reduced calculation cost, compared with the unitary RVOD-RD-MUSIC algorithms developed in [5], as well as their robustness to noise make the developed algorithms very interesting in many applications that require large array size with a few sources such as the case in underwater acoustic.

### 3.5 RD Cramer Rao Bound (RD-CRB)

To evaluate the performances on DoAs estimation of the proposed algorithms through computer simulation, an analytical CRB expression that takes into account the ESPAR antennas particularities is required. Since the frequency-weighted matrix $\boldsymbol{W}$ is independent of the sources DoAs and assumed to be a constant matrix, it can be included in the CRB derivations by replacing the conventional steering matrix $\boldsymbol{A}$ with the new RD-steering matrix $\boldsymbol{A}_{\mathrm{RD}}$. In [5], an expression for the CRB was derived for ESPAR antennas array given as

$$\mathrm{RD-CRB} = \frac{\sigma^2}{2N_s}[(\mathrm{Real}\{(\boldsymbol{D}^{\mathrm{H}}\boldsymbol{P}_{\mathrm{RD}}^{\perp}\boldsymbol{D}) \odot R_s^{\mathrm{T}}\})^{-1}]_{ii} \tag{41}$$

where $\odot$ denotes the Hadamard product and $\boldsymbol{P}_e^{\perp}$ is the orthogonal projector on the null space of $\boldsymbol{A}_{\mathrm{RD}}$ expressed as

$$\boldsymbol{P}_{\mathrm{RD}}^{\perp} = \boldsymbol{I}_{M+1} - \boldsymbol{A}_{\mathrm{RD}}(\boldsymbol{A}_{\mathrm{RD}}^{\mathrm{H}}\boldsymbol{A}_{\mathrm{RD}})^{-1}\boldsymbol{A}_{\mathrm{RD}}^{\mathrm{H}} \tag{42}$$

with $\boldsymbol{D} = (\partial A_{\mathrm{RD}}/\partial\theta) = \boldsymbol{W}^{\mathrm{T}}(\partial\boldsymbol{A}/\partial\theta)$.

## 4 Simulation results

This section reports simulations that have been conducted for performances verification of the proposed algorithms. In the first part, it will be of our interest to validate our approach by studying the precision and the resolution capabilities

under uncorrelated sources scenarios. After that, we will perform other simulations under correlated sources situations to study the behaviour of the proposed algorithms in such scenario.

For RD-signal processing technique, more data CM estimation errors are brought by the directive radiation patterns, which can be viewed as a natural price of the ESPAR antennas advantages compared with the conventional antenna systems as already mentioned in the introduction. Therefore it is very important to verify the ability of the ESPAR antennas shape to form such directive radiation patterns to minimise the data CM estimation errors. An example of the resulting empirical radiation patterns are plotted as a function of the azimuth direction angles in Fig. 2. We can clearly see that our ESPAR antenna is able to form directive radiation patterns that steer their maximum beam at 60°, 120°, 240° and 300°, respectively.

Simulation, as shown in Fig. 3, proves the multiple-signal-resolution capability of the proposed methods. It depicts the resulting spectrums obtained using 2000 snapshots to compute $\widehat{\boldsymbol{R}}_u$ from (19) with 500 independent simulation trials. Three uncorrelated sources, that impinge the ESPAR antennas from 30°, 60° and 90°, respectively, are considered with a SNR level of 30 dB per sources. From the illustrated results, it is clearly seen that all algorithms exhibit selective peaks towards the true DoAs. Particularly, we show that both introduced RVOD techniques can efficiently estimate the propagator operator from the sampled real-valued RD-CM and achieves satisfactory results in DoAs estimation in multiple signal scenarios.

Let us now study the precision in DoAs estimation of these various algorithms. For this purpose we use, as performance parameter, the root-mean-square error (RMSE) defined as

$$\mathrm{RMSE}(\hat{\theta}_k) = \sqrt{\frac{1}{N_s}\sum_{n=1}^{N_s}(\hat{\theta}_k - \theta_k)^2} \tag{43}$$

In Fig. 4, the resulting RMSE on DoAs estimation of two sources located at 25° and 80°, respectively, are plotted as a function of the SNR levels. The RMSE results are averaged over 2000 simulation trials where 5000 snapshots per pattern are used to compute $\widehat{\boldsymbol{R}}_{yy}$ from (9). Fig. 4 shows that the estimation errors, achieved by the developed algorithms, decrease quickly and become closer to the RD-CRB curve as soon as the SNR level increases.

Particularly, this simulation shows that both unit-QR-RD-PM and unit-LU-RD-PM algorithms achieve robust DoAs estimation than both RD-PM and unit-RD-PM algorithms for small SNR levels (noisy situations). This may be because of the fact that the classic propagator method is based on a least square solution that is very sensitive to noise. However, the necessary information of both RVOD-based unit-PM algorithms that enables an accurate DoAs estimation is contained in the upper triangular matrices obtained through $\boldsymbol{LU}$ or $\boldsymbol{QR}$ decomposition. This leads to some improvement on DoAs

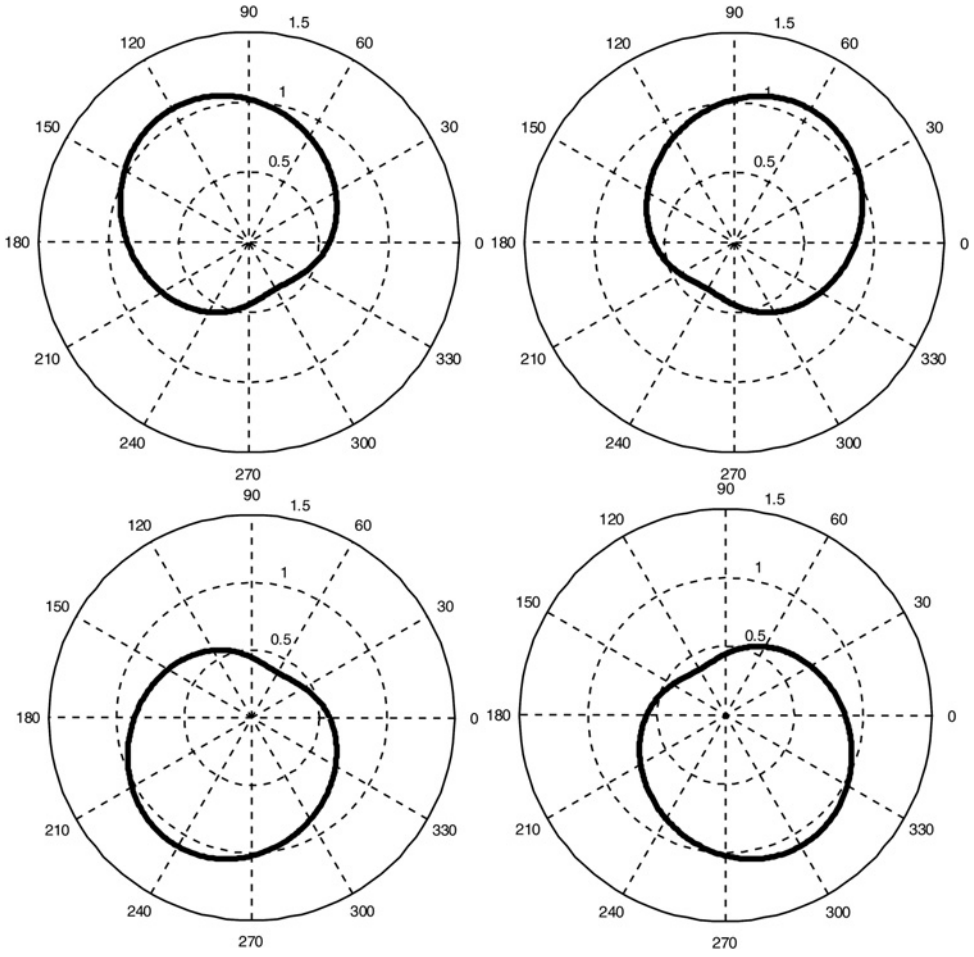


**Fig. 2** *Example of the directive beam patterns used in the simulation*




doi: 10.1049/iet-map.2012.0334

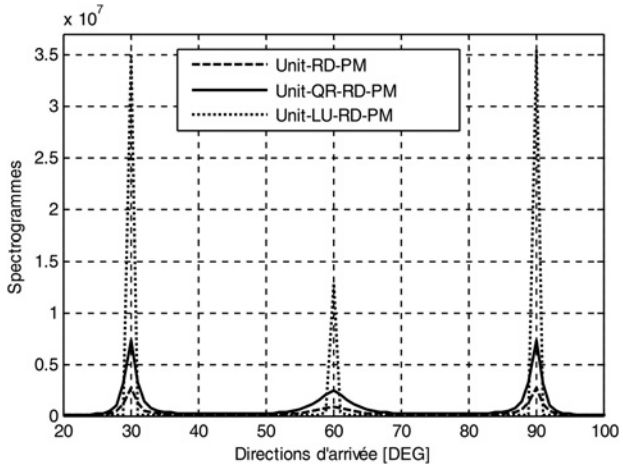


**Fig. 3** *Resulting spectrums as a function of azimuth angles of the three proposed algorithms*

Unit-LU-RD-PM dotted line, unit-QR-RD-PM solid line and the unit-RD-PM dashed line

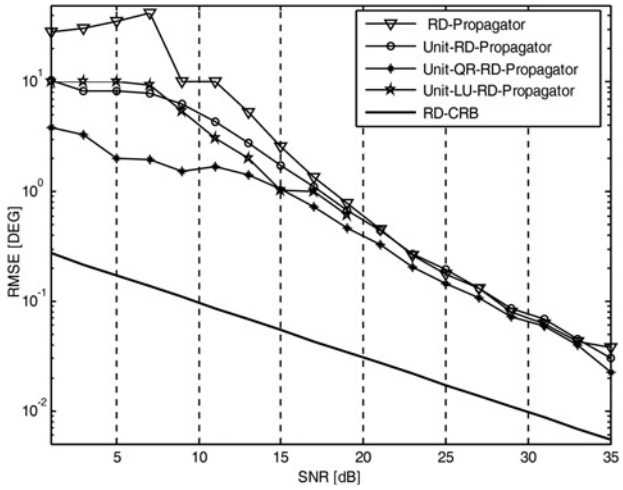


**Fig. 4** *Resulting estimation errors against the SNR levels*

estimation accuracy even in noisy environment. Therefore as Fig. 4 clearly demonstrates, both RVOD techniques can estimate accurately the propagator operator from these upper triangular matrices and achieves more robustness to noise as compared with the classic propagator method. However, in comparison between these two introduced RVOD techniques, it is interesting to point out here that the ***LU*** orthogonal decomposition [9] can reduce the calculation complexity over the ***QR*** decomposition by a factor of two. More precisely, the number of additions and multiplications required by the ***QR*** decomposition is about twice that of using the ***LU*** decomposition. On the other hand, no more digits are required in inexact arithmetic because the numerical stability of the ***QR*** decomposition is guaranteed, which reduces the need to a large memory capacity to store the data.

Simulation shown in Fig. 5 aims at comparing the performances of the proposed algorithms with both RD-CRB (41) and conventional arrays. It exhibits the resulting RMSE on DoAs estimation as a function of the angular separation $\Delta\theta = |\theta_2 - \theta_1|$ when two closely uncorrelated sources impinge the ESPAR antennas with an SNR of 30 dB. The first source has a DoA at $\theta_1$ that

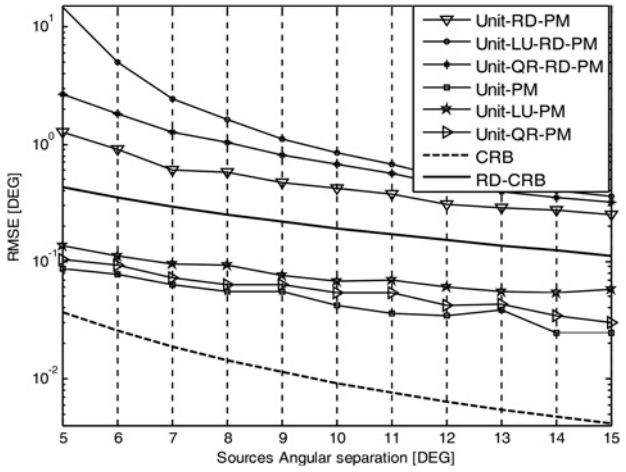


**Fig. 5** *DoAs estimation errors (RMSE) against the angular separation $\Delta\theta$ between two incoming uncorrelated sources*

increases from 65° to 80°; however, the second source has a fixed DoA at $\theta_2 = 60°$. Only the RMSE curve of the first source, obtained with 500 snapshots and averaged over 1000 independent simulation trials, is shown because the other curve has similar behaviour.

The illustrated results show that both unit-RD-PM and unit-QR-RD-PM achieve satisfactory estimation accuracy even for a closely sources' DoAs (less than 1° for $\Delta\theta = 7°$). From Fig. 5, we also show some degradations on the estimation accuracy of the LU-RD-unit-PM for a closely sources DoAs scenario. This may be because of the fact that the ***LU*** decomposition has lower numerical stability than the ***QR*** decomposition as mentioned above.

To further validate our approach, it is interesting to compare the performances on DoAs estimation of our methods achieved with ESPAR antennas with those achieved with conventional antennas arrays. The conventional array is assumed to be perfectly calibrated, so, mutual coupling effects because of $r = \lambda/4$ could be neglected. From Fig. 5, it is clear that conventional array gives better results than ESPAR antennas. However, although such results could be expected, performances of ESPAR antennas can be considered sufficient for DoAs estimation applications in comparison with conventional arrays. Moreover, the cost reduction using only a single active receiver as well as the low-power consumption of the ESPAR antennas may outweigh their performance loss in closely sources DoAs scenario compared with conventional antennas arrays.

Another important criterion for real-time implementation is the required snapshot number (samples) to achieve good DoAs estimation. In practice case, we want to decrease the calculation cost and the time processing as much as possible by working with a small snapshots number. To clearly appreciate the influence of the snapshots number on the performances of the proposed algorithms we summarise, in Table 1, the DoAs estimation values of two incoming uncorrelated signals from 55° and 90°, respectively, obtained through 500 simulation trials with an SNR level of 20 dB per sources. The main goal of those simulations is to compare the achieved performance by the proposed algorithms in a few snapshots scenarios.

Results in Table 1 confirm that both unit-RVOD-RD-PM can perform good DoAs estimation with a small snapshot number. Indeed, with 500 snapshots the estimation error is

**Table 1** Influence of the snapshot number on DoAs estimation

| SNR, dB | RD-PM | | Unit-RD-PM | | Unit-RD-LU-PM | | Unit-RD-QR-PM | |
|---|---|---|---|---|---|---|---|---|
| | 20 | 20 | 20 | 20 | 20 | 20 | 20 | 20 |
| true DoAs, DEG | 55° | 90° | 55° | 90° | 55° | 90° | 55° | 90° |
| estimated DoAs with 50 snapshots | 54.7° | 91.5° | 54.6° | 91.2° | 54.8° | 91.8° | 54.7° | 91.7° |
| estimated DoAs with 500 snapshots | 54.8° | 90.8° | 54.8° | 90.4° | 54.9° | 90.6° | 54.8° | 90.5° |
| estimated DoAs with 5000 snapshots | 55.1° | 90.5° | 54.9° | 90.1° | 55.1° | 90.2° | 54.9° | 90.3° |

about 0.86° that decreases to 0.1° when the snapshots number increases to 5000. Therefore our approach can be considered usable for DoAs estimation since it performs satisfactory results in finite snapshots number scenario.

The last simulation, shown in Fig. 6, aims at studying the DoAs estimation of the proposed algorithms under correlated sources situations. It depicts the resulting RMSE, computed using 50 000 snapshots and averaged over 1000 simulation trials, against the sources correlation coefficient. Two correlated sources, with an SNR of 30 dB, that impinge the ESPAR antenna from 30° and 80°, respectively, are considered.

Again, because of the similarity, the RMSE curve of the incoming source from 30° is only shown and the obtained results are compared with these achieved by the unit-RD-MUSIC and the unit-QR-RD-MUSIC algorithms [5]. We can see that both unit-RD-PM and unit-QR-RD-PM algorithms can prominently distinguish the DoAs of the incoming correlated sources and perform some improvements on DoAs estimation over the unit-LU-RD-PM algorithm for moderately correlated sources scenarios ($0.6 < |\rho| < 0.85$). However, as the sources become fully correlated, ($0.94 < |\rho| < 1$), the illustrated results indicate that all RVOD-based algorithms are failure to estimated the sources' DoAs as compared with the unit-RD-MUSIC algorithm and the unit-RD-PM algorithm. This limitation may be because of the fact that the resulting algorithms without eigendecomposition are approximation methods, so that, its numerical stability degrades quickly when the data CM rank is affected. Nevertheless, Fig. 6 indicates also that all proposed algorithms have approximately the same behaviour for moderately correlated sources scenario ($0.3 < |\rho| < 0.84$). Therefore in comparison between all proposed RVOD-based algorithms, an accurate DoAs estimation can be achieved except when the incoming sources are coherent ($|\rho| = 1$) as it is also the case for both unit-RD-MUSIC and unit-RD-PM algorithms. However, although that may constitute a limitation, the gain in computational load provided by these techniques by using only linear operations, may overcomes their performance loss in coherent sources situations.

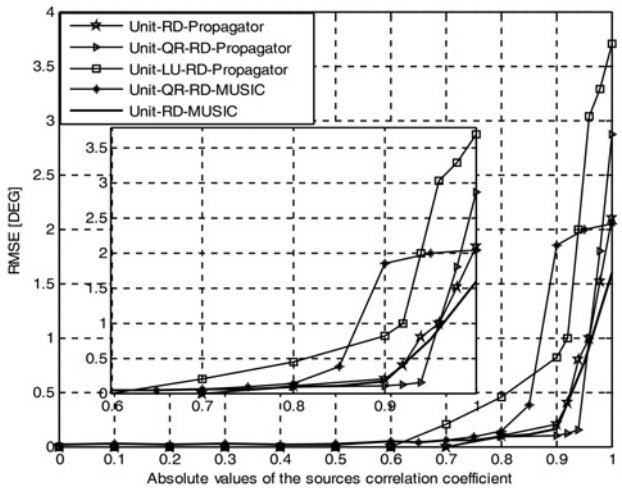


**Fig. 6** *Resulting DoAs estimation errors (RMSE) against the sources correlation coefficient*

## 5 Concluding comments

Based on the classic propagator method, we have developed four algorithms for DoAs estimation of highly correlated signals with an ESPAR antenna. The used real-valued transformation not only yields to a higher resolution capabilities, but also, it considerably reduces the estimator computational complexity, the required data storing capacity and the processing time, which are challenging criteria for a real-time implementation of any DoAs estimator. Furthermore, we also demonstrate that estimating the propagator operator using both introduced orthogonal decomposition techniques enables robust DoAs estimation in noisy environments as compared with the classic propagator algorithm. Moreover, the performances of the proposed algorithms are compared with both CRB and conventional arrays in terms of the angular resolution ($\Delta\theta$) and good behaviours are illustrated. In addition, although that both resulting RVOD-based algorithms are an approximation methods, the numerical results show its high accuracy especially for a low SNR levels. On the other hand, the conducted simulations also show that the performances of all proposed algorithms are close enough to the CRB to be considered sufficient for DoAs finding applications.

## 6 References

1 Schmit, O.R.: 'Multiple emitter location and signal parameters estimation', *IEEE Trans. Antennas Propag.*, 1986, **34**, pp. 276–280
2 Roy, R., Kailath, T.: 'ESPRIT-estimation of signal parameters via rotational invariance techniques', *IEEE Trans. Acoustic Speech Signal Process.*, 1989, **37**, (7), pp. 984–995
3 Marcos, S., Marsal, A., Benidir, M.: 'The propagator method for source bearing estimation', *Signal Process.*, 1995, **42**, pp. 121–138
4 Munier, J., Delisle, G.Y.: 'Spatial analysis using new properties of the cross spectral matrix', *IEEE Trans. Signal Process.*, 1991, **39**, (3), pp. 746–749
5 Akkar, S., Gharsallah, A.: 'Reactance domains unitary MUSIC algorithms based on real valued orthogonal decomposition for ESPAR antennas', *IET Microw. Antennas Propag.*, 2012, **6**, (2), pp. 223–230
6 Plapous, C., Cheng, J., Taillefer, E., Hirata, A., Ohira, T.: 'Reactance domain MUSIC algorithm for electronically steerable parasitic array radiator antenna', *IEEE Trans. Antenna Propag.*, 2004, **52**, (12), pp. 3257–3264




doi: 10.1049/iet-map.2012.0334

7 Taillefer, E., Nomura, W., Cheng, J., Taromaru, M., Watanabe, Y., Ohira, T.: 'Enhanced reactance-domain ESPRIT algorithm employing multiple beams and translational-invariance soft selection for direction-of-arrival estimation in the full azimuth', *IEEE Trans. Antennas Propag.*, 2008, **56**, (8), pp. 2514–2526
8 Han, Q., Hanna, B., Inagaki, K., Ohira, T.: 'Mutual impedance extraction and varactor calibration technique for ESPAR antenna characterization', *IEEE Trans. Antennas Propag.*, 2006, **54**, (12), pp. 3713–3720
9 Fargues, M.P., Ferreira, M.P.: 'Investigations in the numerical behavior of the adaptive rank-revealing *QR* factorization', *IEEE Trans. Acoustics Speech Signal Process.*, 1955, **43**, pp. 2787–2791
10 Bischof, C.H., Shroff, G.M.: 'On updating signal subspaces', *IEEE Trans. Acoustics Speech Signal Process.*, 1992, **40**, pp. 96–105
11 Miranian, L., Gu, M.: 'Strong rank revealing LU factorizations', *Linear Algebra Appl.*, 2003, **367**, pp. 1–16
12 Wax, M., Kailath, T.: 'Detection of signals by information theoretic criteria', *IEEE Trans. Acoustic Speech Signal Process.*, 1985, **33**, pp. 387–392
13 Linebarger, D.A., DeGroat, R.D., Dowling, E.M.: 'Efficient direction finding methods employing forward/backward averaging', *IEEE Trans. Signal Process.*, 1994, **42**, (8), pp. 2136–2145
14 Haardt, M., Nossek, J.A.: 'Unitary ESPRIT: how to obtain increased estimation accuracy with a reduced computational burden', *IEEE Trans. Signal Process.*, 1995, **43**, (5), pp. 1232–1242
15 Hnarng, K.C., Yeh, C.C.: 'A unitary transformation method for angle-of-arrival estimation', *IEEE Trans. Signal Process.*, 1991, **39**, pp. 975–977
16 Lutkepohl, H.: 'Handbook of matrices' (John Wiley & Sons', 1996)
17 Stoica, P., Jansson, M.: 'On forward–backward MODE for array signal processing', *Digital Signal Process.*, 1997, **7**, (4), pp. 239–252